RESEARCH ARTICLE

Using Biomimetics to Mimic Bamboo to Create a More Robust and More Durable Material

Sean Jung

Punahou School, 1601 Punahou St, Honolulu, HI 96822, USA; seanminjung@gmail.com
Mentor: Dr. Jong Seol Jeong

ABSTRACT: Through biomimetics, numerous contraptions and inventions inspired by nature and its processes have revolutionized the world. A quick pan around any room will reveal an abundance of cylindrical tubes or rods. Whether it is used in construction equipment or holding up large, heavy structures, the sheer quantity of the cylindrical tube begs for improvement. Nature's cylindrical tube is the bamboo plant. Bamboo plants are durable and have extreme structural and tensile strength. The source of the bamboo's strength is a diaphragm or node. Three specimen types with varying frequencies and numbers of diaphragms were synthesized and tested. We hypothesize that placing "diaphragms" in tubes would increase the structural strength of the tube as a whole. We also hypothesize that more diaphragms would increase overall structural strength. Experiment results are consistent with the hypothesis. There is a drastic difference in tensile and compressive strength between a tube with no diaphragm and one with one. However, interestingly, adding more diagrams only increases the structural strength marginally. It is likely that, like the bamboo plant, the perfect ratio of diaphragms is the strongest the tube could ever be.

KEYWORDS: Materials Science; Biomimicry; Biomimetics; Bamboo; Diaphragm.

Introduction

Since the dawn of human civilization, humans have been constructing marvelous inventions and contraptions that have benefited our species dramatically. Though we may credit Leonardo DaVinci or Thomas Edison as the greatest inventors of all time, mother nature is the most significant inventor.[1,2] While we may have gone from the wheel to the Metaverse in a couple of thousand years,[3] nature has constantly evolved for billions of years. While humanity was in its infancy, nature had built up billions of years of research and development that natural selection coaxed out.[4,5] This means scientists can look back into nature to determine how we could copy and use it to our advantage. We call this concept ***biomimetics***.[6,7]

According to the Oxford Dictionary, biomimicry is the design and production of materials, structures, and systems mimicking biological entities and processes. Though we may not realize it, countless crucial inventions that improve our lives daily are the outcome of what nature inspires.[8] During the 1990s in Japan, Japanese scientists and engineers were looking to make their trains faster and more efficient. As it turned out, speed came with one main problem: sound.[9] A deafening sonic boom was heard throughout the surrounding areas when the trains exited tunnels at high speeds.[10-12] Puzzled, one of the Japanese scientists looked to nature to find the key. As the story goes, while observing the Kingfisher bird hunt for fish in the lake, the Japanese scientist was hit with a realization.[13] As he observed, the Kingfisher bird could enter the water with little sound not to scare its prey away. After several experiments, the scientist found that the beak of the Kingfisher bird allowed it to break the water's surface with minimal resistance. By applying the design of the Kingfisher bird's beak onto a train, the Japanese scientists found that the noise was drastically lower.[14] To this day, the bullet train glides at speeds up to 320 km/hour (Figure 1).[15]

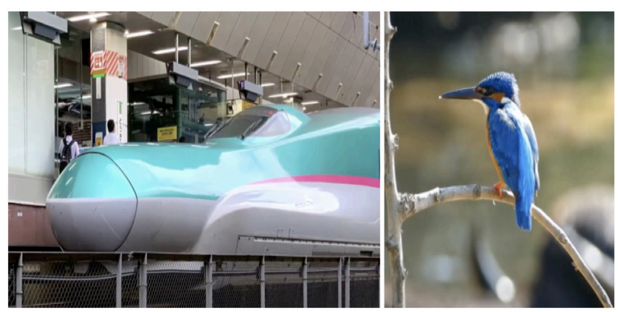

Figure 1: Using biomimicry in building and developing Japan's famous bullet train.

Furthermore, in the case of military aircraft, speed is also an essential factor. Though the Wright Brothers have been up in the air hundreds of years ago, nature has been creating aircraft of its own.[16] The B-2 Stealth Bomber is a military aircraft that mimics the world's fastest animal on earth: the Peregrine Falcon.[17] Similarities are apparent when comparing the B-2 Stealth Bomber and the Peregrine Falcon side-by-side comparison. The Stealth Bomber has a similar "head" shaped portion near the cockpit, while its wings mirror those of a fully extended Peregrine Falcon (Figure 2).[18]

DOI: 10.36838/v5i6.20

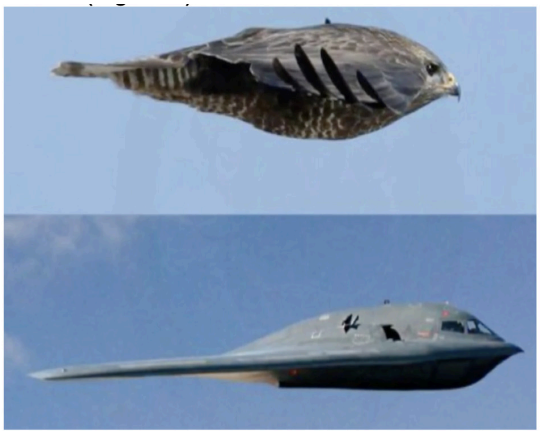

Figure 2: The United States military developed the Northrop Grumman B-2 Spirit, or the Stealth Bomber, to mimic the fastest animal in the world: the Peregrine Falcon.

Every day scientists search for new and inventive ways to incorporate biomimicry into our lives.[19,20] Like any inventor will say, however, the first step in solving a problem is identifying that there is one in the first place. A quick scan around any room will reveal that rods or bars are a big part of our daily lives. Whether the bars holding up a table or the rods holding up construction workers, cylindrical shapes are a crucial part of daily living.[21,22] With such an essential role in our lives, it is evident that the safety of these bars is also necessary. We professionally describe this bar shape as a cylindrical rod. When manufacturing equipment, structural integrity is crucial.[23] This is especially true in scenarios where the health and safety of people are at stake.[24,25] With this in mind, the question is how the cylindrical rod could be improved in terms of structural strength to benefit us.

The bamboo plant is the most remarkable example of a cylindrical rod in nature. During the end of the second world war, the United States had created a bomb so powerful that they believed it could end the war that had claimed millions of lives.[26] Pushing closer and closer to the mainland of Japan, the United States military did not find evidence that the Japanese were slowing down.[27] With the permission of President Harry S. Truman, the U.S. detonated two atomic bombs on Hiroshima and Nagasaki.[28,29] Though every free-standing structure was obliterated, bamboo groves stood proud and tall. Even through immense stress and pressure, the bamboo plant withstood it all, which is no surprise, as bamboo is flexible.[30] It possesses an outer surface that is strong and dense, but as you go in, the density gets lower but stays durable and enduring.[31] This is why it bends well and absorbs external force. Bamboo is highly elastic and has a higher tensile strength than some alloys.[32] Bamboo has higher compressive strength than many mixtures of concrete. For this very reason, people use bamboo to assist construction workers in many countries in Asia, primarily Southeast Asia.[33,34]

With this data in mind, using biomimicry, bamboo's structural strength could be synthesized and applied to modern science to create stronger, more durable materials. Bamboo gets its unique strength from the "nodes" placed intricately throughout its internal structure. These nodes are disc-shaped. Scientists call these "diaphragms" (Figure 3).

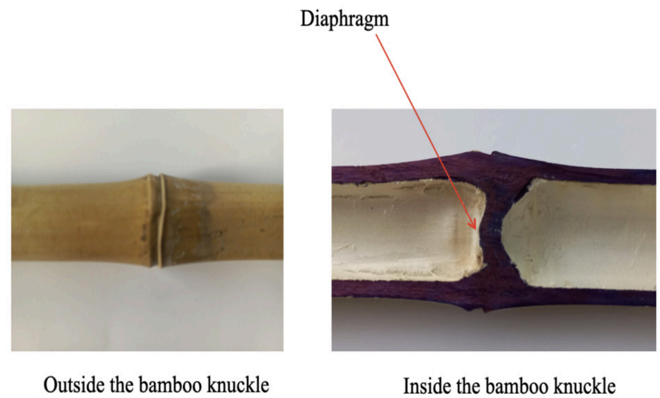

Figure 3: Bamboo's external surface is hard and durable. On the outside of the bamboo, there is a "knuckle." This knuckle bares a striking resemblance to the human knuckle. On the internal surface of the bamboo, there is a disc called the "diaphragm." This diaphragm is a circular node located on the inner surface of the bamboo.

Based on the previous research,[35-37] this study examined whether placing "diaphragms" in tubes would increase the structural strength of the tube as a whole. With cylindrical shapes so prevalent in our lives, this study contributes to the research and development of everything, which includes rods and tubes. From construction equipment to pull-up bars to NASA spacecraft,[38] the structural integrity of such objects is crucial to the safety of everyone around and using them. Furthermore, we can save money and resources by making rods more structurally strong without making solid rods, which can lead to environmental and economic benefits.[39]

Research Question and Hypothesis:

The research question asked is: "How could the structural strength of a bar be improved by synthesizing the biomimicry of bamboo?" We hypothesize that placing "diaphragms" in tubes would increase the structural strength of the tube.[40,41] It was further hypothesized that more diaphragms would increase overall structural strength. More specifically, a tube with three diaphragms would be more structurally stable than a tube with one diaphragm and a tube without any diaphragm. Furthermore, by the same logic, the tube with one diaphragm would be more robust than a tube without any diaphragm.

■ Methods

Study Sites:

We collected data from the experiment performed at the Seoul National University of Science and Technology research laboratory. We chose this location due to its access to the INSTRON tensile, compression, fatigue, impact, rheology, and structural testing machine (Figure 4).

Figure 4: The INTRON 4467 machine performing the three-point bending test.

Experimental Design:

Using the INSTRON tensile, compression, fatigue, impact, rheology, and structural testing machine, a "three-point bending test" was performed.[42,43] The "three-point bending test" is designed to test the structural strength of a given specimen. As two pillars held up the specimen, a third pillar was lowered into the middle, adding weight to the tube until it fractured. We refer to the two pillars that held up the specimen as "supporting anvils" and refer to the third as the "load anvil" (Figures 5 and 6). Using the "three-point bending test," both compressive and tensile stresses were measured. As the INSTRON 4467 loaded on weight via the "load anvil," the structural strength was recorded and collected (Figure 5).

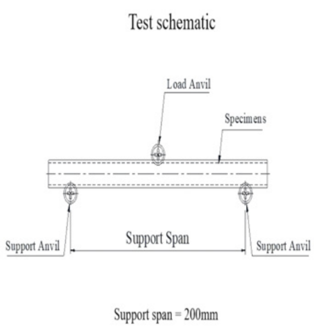

Figure 5: Inner workings of the three-point bending test.[44]

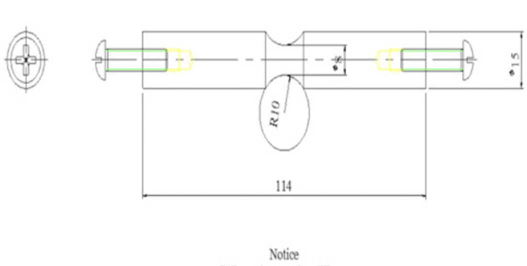

Figure 6: The load and support anvils of the INSTRON 4467 Tensile Testing machine are identical and contain a 'divot' in the center where we locate the specimen. The 'divot' is made for the specimen to fit precisely for the three-point bending test.

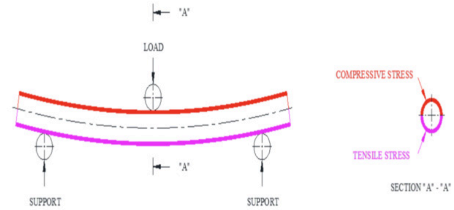

Figure 7: The three-point bending test shows two types of stress on the specimen. On the lower side of the specimen, tensile stress (σbt) occurs, while compressive stress (σbc) occurs on the upper side. Tensile stress is the stress that causes the length of the specimen to increase, while compressive stress is the stress that causes the length of the specimen to decrease.[45]

Three types of specimens were developed and tested. We made the body of each specimen out of a standard clear, plastic, acrylic pipe (PMMA, Poly methyl methacrylate). We used the same material to construct the diaphragms inside each specimen. The three types of specimens vary in frequency and distance of diaphragms - Type 00, Type B1, and Type B3. While Type 00 is just a pipe with no diaphragm, Type B1 and B3 contain one and three diaphragms, respectively. All pipes are 250 mm in length and 20 mm in diameter. The internal diameter of the pipes is 16 mm across. Type 00 is an empty acrylic pipe 250 mm long (Figure 8). In Type B1, one singular diaphragm in the center equidistant from the sides is located precisely in the middle or 125 mm from each edge (Figure 9). In Type B3, there are three diaphragms. One is directly in the center, and two are 100 mm from the center (Figure 10). Each diaphragm is 16 mm in height and 8 mm in length (Figure 11). To reduce the effect of measurement errors on experiment results, we made five specimens for each type, thus, 15 specimens.

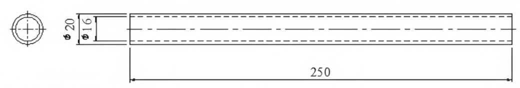

Figure 8: Type 00 specimen design consists of an empty acrylic plastic tube with no diaphragm. It is 250 mm in length and 20 mm in diameter. The internal diameter of the pipe is 16 mm across.

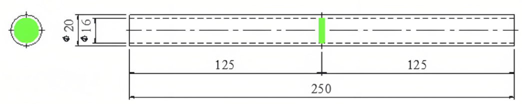

Figure 9: Type B1 specimen design consists of an acrylic plastic tube with one diaphragm. One singular diaphragm in the center equidistant from the sides is located precisely in the middle or 125 mm from each edge. It is 250 mm in total length and 20 mm in diameter. The internal diameter of the pipe is 16 mm across.

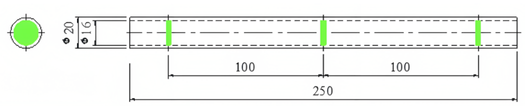

Figure 10: Type B3 specimen design consists of an acrylic plastic tube with one diaphragms. One is directly in the center, and two are 100 mm from the center. It is 250 mm in total length and 20 mm in diameter. The internal diameter of the pipe is 16 mm across.

DOI: 10.36838/v5i6.20

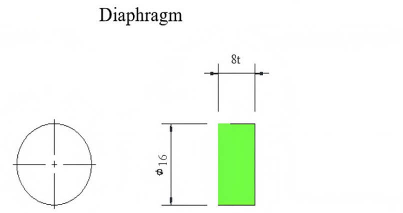

Figure 11: Each diaphragm is 16 mm in height and 8 mm in length..

We collected data from the testing device INSTRON 4467 (3 tons) at pressure speeds of 2 mm per minute. The support span of the INSTRON 4467 is 200 mm. The lab's temperature at the time of testing was 27~29°C (80.6~84.2℉), with a lab humidity of 62~64%.

Results and Discussion

Results:

As mentioned, five specimens were made for each type – TYPE 00, TYPE B1, and TYPE B3 to reduce measurement errors in experimental results. Since we inserted one diaphragm for TYPE B1 and three diaphragms for TYPE B3, specimens for TYPE B1 and TYPE B3 are heavier than those for TYPE00. We report these results in Table 2 below (column entitled 'weight of tube').

The INSTRON 4467 machine produced data on the maximum force endured by each specimen in both kg (kilograms) and N (newtons). We calculated the maximum tensile and compressive stress values to test hypotheses using this data. From the point where the load anvil touches each specimen, we could identify each specimen's maximum compressive and tensile stress points. The side of the load anvil is called the maximum compressive stress point, and the opposite side is called the maximum tensile stress point (in Figure 12).

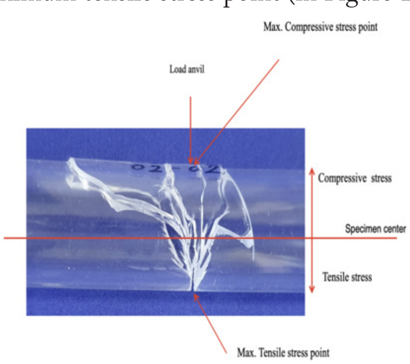

Figure 12: The fracture point on the lower side of the specimen is called the maximum tensile stress point. The point where the load anvil weighs on the specimen is called the maximum compressive stress point.

The values for maximum bending moment, M_{max}, were first needed to get the values of these stresses. To calculate M_{max}, the following equation is used (in Figure 13).[45] We computed the maximum bending moment, M_{max}, by multiplying the distance between the support anvil and the center of the specimen (i.e., the half of the support span), or L/2, and load, the pressure of load anvil (P). Since each half of the specimen experiences half of the load (= P/2), M_{max} = P/2*L/2 = P*L/4. The bottom panel of Figure 13 graphically shows how P and L are defined.

$$M_{max} = \frac{P * L}{4}$$

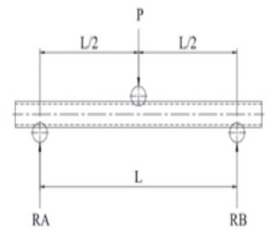

Figure 13: Equation to calculate maximum bending moment, M_{max}[45].

$$\sigma_{bt}, \sigma_{bc} = \frac{M_{max} * y}{I_x}$$

$$I = \frac{\pi}{I_x}(d_0^4 - d_i^4),$$

where d_o = specimen outside diameter and d_i = specimen inside diameter

Figure 14: We show the equation to calculate the maximum tensile and compressive stresses on the top.[49] While both maximum tensile (σ_{bt}) and compressive stresses (σ_{bc}) have the same magnitude, their signs are opposite - the maximum tensile stress (σ_{bt}) has a positive value, and the compressive stress (σ_{bc}) has a negative value. Finally, we show the formula to calculate the moment of inertia (Ix) used in computing maximum tensile and compressive stresses on the bottom.

Then, as shown in Figure 14, both maximum tensile and compressive stresses are computed by multiplying the maximum bending moment (M_{max}) and the coordinate from the center of the specimen (y) divided by the moment of inertia (I_X). Since all specimens are identical in length and location in the testing machine, by experimental design, y should be the same for all types of specimens. While the value of I_X should be different theoretically for each type due to the existence and frequency of diaphragms, the difference in I_X between types is statistically insignificant in this experiment, potentially due to the nature of the material for specimens (i.e., plastic). In addition, the difference is too small to be detected by the testing machine. Thus, we assume that those values are the same for all types. Therefore, according to the equation below, since the coordinate from the center of the specimen (y) and the moment of inertia (I_X) remain the same for all the types, as the maximum bending moment (M_{max}), the numerator of the equation increases, the maximum tensile (σ_{bt}) and compressive stresses (σ_{bc}) increase.

Figure 14 shows how to calculate the moment of inertia (Ix) based on the formula.[45] As explained, the outside diameter of the specimen is 20mm, and the inside diameter of the specimen is 16mm. Pi is simplified to be 3.14. Plugging these numbers in the equation, the value of inertia (I_X) is 4,636.91 throughout all specimens in the experiment. We used this value when calculating the maximum tensile (σ_{bt}) and compressive stresses (σ_{bc}).

Table 1 below shows how to calculate the maximum bending moment and maximum tensile and compressive stresses based on results obtained from the experiment for the TYPE 00 - specimen without a diaphragm. For the value, P, also known as the maximum load, the average maximum load of all five Type 00 specimens is used in the units Newton (= the absolute unit of force in the International System of Units), which is 683.2 L (= support span), y (= the coordinate from the center of the specimen), and I_X (= the moment of inertia), remain the same for all the types. In this example, we plugged 200.0 for L, 10.0 for y, and 4,636.9 for I_X, respectively, in the equations to compute the maximum bending moment and maximum tensile and compressive stresses. After computations, 34,160.0 N.mm and 73.7 MPa were obtained for maximum bending moment and maximum tensile and compressive stresses, respectively, for Type 00 (specimen without a diaphragm).

Table 1: Example calculating maximum bending moment and maximum tensile and compressive stresses for TYPE 00.

1. Design Data

1)	Load	P	=	660.0	N	=	67.4	kg
2)	Support Span	L	=	200.0	mm			
3)	Tensile Strength of PMMA	σ_{max}	=	71.0	MPa	=	723.9	kg/cm²
4)	Specimens Out Dia.	D	=	20.0	mm			
5)	Specimens In Dia.	d	=	16.0	mm			
		y	=	10.0	mm			
6)	2nd Moment of Area(I_x)	I_x	=	4,636.9	mm⁴			
7)	Reaction force $R_A = R_B$	$R_A = R_B$	=	330.0	N	=	33.7	kg

2. Moment

1) Maximum Bending Moment

$$M_{max} = \frac{P * L}{4} = \frac{660.0*200.0}{4} = 33{,}000.0 \quad N \cdot mm$$

3. Stress

1) Maximum Tensile & Compressive Stress (σ_{bt}, σ_{bc})

$$\sigma_{bt}, \sigma_{bc} = \frac{M_{max} * y}{I_x} = \frac{33{,}000.0*10.0}{4{,}636.9} = 71.2 \quad MPa$$

In the same way, we computed the values for the maximum bending moment and maximum tensile and compressive stresses of all types of specimens. As explained, since support span (= L), the coordinate from the center of the specimen (= y), and the moment of inertia (= I_X) are constant for all types, P (maximum load) determines the values of maximum bending moment and maximum tensile and compressive stresses. For Type B1, the testing machine generated the value of 908.5 N, on average, for P (= maximum load). For Type B3, the value of P is 923.5 N. Table 2 summarizes all the results based on the above equations.

Table 2: Data to calculate the values of all types' maximum bending moment and maximum tensile and compressive stresses.

TYPE	Specimen number	Maximum load (kg)	Average maximum load (kg)	Maximum load (N)	Average maximum load (N)	Weight of specimen (g)	$I_x(mm^4)$	y(mm)	M_{max}	σ_{max}(MPa)
TYPE 00	00-01	70	69.7	686.47	683.2	34.355	4,636.99	10	34,159.8	73.7
	00-02	75		735.50		34.454				
	00-03	64		627.63		32.724				
	00-04	65		637.43		32.862				
	00-05	74		725.69		34.390				

TYPE	Specimen number	Maximum load (kg)	Average maximum load (kg)	Maximum load (N)	Average maximum load (N)	Weight of specimen (g)	$I_x(mm^4)$	y(mm)	M_{max}	σ_{max}(MPa)
TYPE B1	B1-01	88.27	92.6	865.63	908.5	36.131	4,636.99	10	45,424.4	98.0
	B1-03	89.31		875.83		35.997				
	B1-04	95.03		931.93		36.005				
	B1-05	93.58		917.71		35.659				
	B1-06	98.82		969.09		36.046				

TYPE	Specimen number	Maximum load (kg)	Average maximum load (kg)	Maximum load (N)	Average maximum load (N)	Weight of specimen (g)	$I_x(mm^4)$	y(mm)	M_{max}	σ_{max}(MPa)
TYPE B3	B3-01	91.89	94.2	901.13	923.5	39.920	4,636.99	10	46,176.2	99.6
	B3-02	96.24		943.79		39.633				
	B3-03	94.39		925.65		39.807				
	B3-04	102.12		1001.46		39.627				
	B3-05	87.22		855.34		39.385				

Results in Table 2 show that the average maximum load for TYPE 00 is 69.7kg or 683.2 N (Newton). Consistent with the hypothesis, the results show that the average maximum load for TYPE B1 is much higher than that for TYPE 00. Since the maximum load is the most critical determinant of both maximum bending moment and maximum tensile and compressive stresses, and the higher maximum load indicates structural strength, these results support the hypothesis. Specifically, the average maximum load based on five specimens of TYPE B1 is 92.6kg, which increases by 32.9% (= (92.6 – 69.7)/69.7, or 908.5 N, which increases by 33% (= (908.5 - 683.2)/683.2), compared to TYPE 00. This increase of approximately 33% in the average maximum load appears meaningful. Furthermore, the average maximum load for TYPE B3 is 94.2 kg or 923.5 N, which is higher than those for both TYPE 00 and TYPE B1. However, the increase in the average maximum load for TYPE B3, relative to TYPE B1, seems to be marginal, considering that TYPE B3 has three diaphragms while TYPE B1 has only one diaphragm.

More importantly, we found similar results when comparing maximum bending moment (M_{max}) and maximum tensile and compressive stresses (σ_{max}(MPa)) among specimens of three types. Specifically, maximum tensile and compressive stresses (σ_{max}(MPa)) for TYPE B1 increase by 33% relative to TYPE 00. Maximum tensile and compressive stresses ((σ_{max}(MPa)) for TYPE B3 are increased by 35.2% relative to TYPE 00. Again, the difference in maximum tensile and compressive stresses ((σ_{max}(MPa)) between TYPE B1 and TYPE B3 do not appear significant. Inferences based on the maximum bending moment (M_{max}) are similar.

The fracture points for each type of specimen were also examined since this examination may corroborate inferences from Table 2. Figure 15 contains photos of the fracture points for each type. It becomes apparent that the fracture in the specimen of TYPE 00 is the most severe (on the left side of Figure 15). On the contrary, the fractures of both TYPE B1 and TYPE B3 are not as severe (on the middle and the right sides of Figure 15).

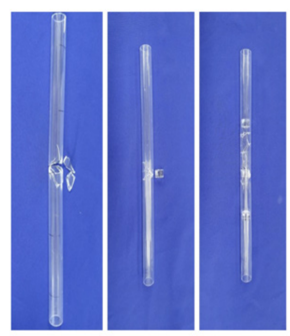

Figure 15: The fracture points for each type are different. The fracture in TYPE 00 is the most severe. On the contrary, the fractures of both TYPE B1 and TYPE B3 are not as severe.

Discussion

Interestingly, there is no significant improvement in structural integrity from one diaphragm to three diaphragms. We like to explore why this is the case further. Structural integrity should increase with more diaphragms, but the marginal increases from adding more diaphragms may decrease. One plausible reason for these results may be the length of the specimen. Due to the size of the INSTRON 4467 Tensile Tester device, the maximum length of each specimen was 250 mm. In the future, we would like to test the effect of length

DOI: 10.36838/v5i6.20

on each specimen variation's tensile strength and durability. Increasing the length proportionately to the number of diaphragms in a specimen would generate more consistent results with the hypothesis - more diaphragms increase the structural strength proportionately. Looking back into nature, we see that bamboo follows a similar pattern. As it grows, bamboo stays consistent with the length between each diaphragm. Mimicking nature in that way may yield a more favorable outcome toward the hypothesis. At the same time, these results provide intriguing implications - simply adding more diaphragms does not significantly improve the structural strength.

Considering the cost of diaphragms, finding an optimal number of diaphragms in the given length is essential. To address this, we plan to design and develop fourth and fifth types of specimens, namely Type B4 and Type B5. Type B4 has four diaphragms with an even spread of diaphragms in a tube. Type B5 contains five diaphragms, and in this type, we will add two more diaphragms to the end of each side of Type B3 (specimen with three diaphragms). Testing hypotheses with these new types of specimens will shed more light on this research question.

We made each specimen out of acrylic plastic tubing due to the budget and manufacturing difficulties when this project started. In the future, we also like to test metal's tensile strength and structural integrity instead of plastic. Since we make most cylindrical tubes used in real life out of metal, these results would yield a more valuable diagnosis of the effect of diaphragms. Testing whether what we found with the plastic tubes is also applied to metal would be very intriguing. Considering that metal is already strong, it is also possible that the results - more diaphragms improve the strength of plastic tubes - may not exist with metal.

To mimic bamboo more closely, we also like to create more similar diaphragms to the ones in real life. For example, when splitting bamboo down the middle, one can observe that the diaphragms of bamboo are not entirely straight and perpendicular to the cylindrical tube. In the future, we would like to design a specimen that more closely mimics the angle and shape of natural bamboo (Figure 3). In addition, on the outside of the bamboo plant, there is a "knuckle": a thicker portion of the plant in the diaphragms' external surface. We also want to mimic this knuckle and test how much strength this knuckle can provide with diaphragms combined.

We also need to test whether a rod with diaphragms is more robust (or equally strong) than a solid rod to compare the tensile strength of specimens used in this project with that of a solid rod. Again, this test could have substantial real-world implications. For example, we can make rods with less material but more or similar structural strength. In that case, they will require less money and resources, leading to positive economic and environmental outcomes.

Conclusion

This paper used biomimicry to improve the cylindrical rod's structural strength. While we can see many solid cylindrical rods in real life, there are also many tube-type, empty cylindrical rods. If we can make tube-type cylindrical rods as strong as solid ones, we can reduce the material costs to make solid cylindrical rods. Considering a recent supply chain disruption in many natural resources due to Covid-19, this research is critical and can significantly contribute to the economy and society. In addition, by reducing materials to make products of cylindrical rods, this research can also significantly contribute to protecting our environment.

Natural characteristics of bamboo are adopted to make empty cylindrical rods stronger. Bamboo is robust due to its diaphragms. Thus, we are interested in how much adding diaphragms can increase the structural strength of empty tubes. Therefore, we hypothesized that a tube with one diaphragm would be more robust than that without one. We also hypothesized that the more diaphragms a tube has, the greater its structural strength is. To test this hypothesis, we made three plastic tube types – a tube without a diaphragm, a tube with one diaphragm, and a tube with three diaphragms and five specimens for each type.

Consistent with the hypothesis, experiment results show that adding diaphragms to an empty tube does improve the structural integrity and tensile strength of a cylindrical tube. However, interestingly, there are non-significant changes in structural integrity between three diaphragms and one diaphragm. Specifically, both TYPE B1 (i.e., a tube with one diaphragm) and TYPE B3 (i.e., a tube with three diaphragms) are more robust than TYPE 00 (i.e., a tube without a diaphragm). However, when comparing TYPE B1 and TYPE B3, the difference is insignificant, based on average maximum load and maximum tensile and compressive stresses. While the average maximum load for TYPE B3 is higher than that for TYPE B1, the increase is only 1.7% (= (94.2-92.6)/92.6). These results suggest a possibility that there is an optimal number or ratio of diaphragms in the given length to maximize the structural strength.

Acknowledgments

We are grateful for the help of the Seoul National University of Science and Technology research laboratory for allowing us to use the INSTRON 4467 Tensile Tester they possess. More specifically, Sean Jung would like to thank Dr. Jong Seol Jeong for his guidance and assistance in allowing him to conduct and explore this experiment. Sean Jung would also like to acknowledge Mr. Johannes Adams for his help in getting me involved in this science fair. Finally, Sean Jung would like to thank the Hawaii Academy of Science for listening and giving him a platform to share his passion for science.

References

1. Benyus, J. Biomimicry: Innovation Inspired by Nature. Harper Co llins Publisher. 2002.
2. Tittmann, B.R.; C.J. Bryan. Biomimicry: Using nature as a model for design. *ACS Central Science.* 2019. *5*(11), 1805-1816.
3. Ansary, T. The Invention of Yesterday: A 50,000-Year History of Human Culture, Conflict, and Connection. *Public Affairs*. 2019.
4. Wade, M.J.; S. Kalisz. The causes of natural selection. *Evolution*. 1 990,44(8),1947–1955.DOI:https://doi.org/10.1111/j.1558-5646. 1990.tb04301.x
5. French, M. Invention and evolution. Cambridge University Press. 1994.

6. Vincent, J. F.V.; O.A. Bogatyreva; N.R. Bogatyrev; A. Bowyer; A-K. Pahl. Biomimetics: its practice and theory. *Journal of the Royal Society Interface*. 2006. DOI: https://doi.org/10.1098/rsif.2006.0127
7. Barthelat, F. Materials by design: lessons from nature. *Advanced Materials*, 2016. 28(24), 5187-5189.
8. Bar-Cohen, Y. Biomimetics – using nature to inspire human in novation. *Bioinspiration and Biomimetics*. 2006, 1(1).
9. Hargroves, K.; M.H. Smith. Innovation inspired by nature biomimicry. *Ecos*. 2006,129.
10. Liu, B.; C. Li; J. Li. Numerical Study of Pressure Waves Generated by High-Speed Train Entering and Exiting Tunnels. *Journal of Fluids and Engineering*. 2017, 139, 011106-1-011106-12.
11. Fan, J.; J. Xie.; H. Chen. Aerodynamic Performance of High-Speed Trains Entering and Exiting Tunnels. Proceedings of the Institution of Mechanical Engineers, Part F: *Journal of Rail and Rapid Transit*. 2014, 228, 255-265.
12. Yoshida, Y.; T. Iida. The aerodynamic design of high-speed trains for tunnel safety and comfort. *Journal of Wind Engineering and Industrial Aerodynamics*, 2015, 145, 126-133.
13. Lee, D. Biomimicry: Inventions Inspired by Nature. Kids Can Press. 2011.
14. Dicks, H. The Biomimicry Revolution: Learning from Nature How to Inhabit the Earth. United States: Columbia University Press. 2023.
15. AskNature. High-Speed Train Inspired by the Kingfisher. The Biomimicry Institute. 2021. Obtained from https://asknature.org/innovation/high-speed-train-inspired-by-the-kingfisher/.
16. Wu, F., A. Han, W., Jiang, Y., Yue, and D. Xie. A biomimetic design of steam turbine blade to improve aerodynamic performance. *International Journal of Thermal Science*. 2022, 181, DOI: https://doi.org/10.1016/j.ijthermalsci.2022.107782
17. Levine, J. The fastest animals in the world. Cell Mentor from Cell Press and Cell Signaling Technology. 2016.
18. Magazine, Smithsonian. How Biomimicry Is Inspiring Human Innovation. Smithsonian.com, Smithsonian Institution, obtained from 1 Sept. 2012, https://www.smithsonianmag.com/science-nature/how-biomimicry-is-inspiring-human-innovation-17924040/.
19. Speck, T.; O. Speck. Biomimetics in architecture: architecture of life and buildings. Springer. 2016.
20. Bhushan, B. Biomimetics: lessons from nature - An overview. *Philosophical Transactions of the Royal Society A: Mathematical, cal, Physical and Engineering Sciences.* 2016, 374(2063).
21. Hecht, E. E.; Cree, G. S. The role of cylindrical objects in human culture and evolution. *Journal of Cognition and Culture*. 2015, 15 (1-2), 1-26.
22. Cho, K. H.; J.H. Lee. Cylindrical objects in everyday life. *International Journal of Industrial Ergonomics*, 2008, 38(7-8), 578-585.
23. Kusiak, A.; J. Wang. Structural Integrity and Failure Prevention in Manufacturing Processes. *Journal of Manufacturing Systems*. 2011, 30(3), 144-152.
24. Lourenço, P. B.; G. Milani. Structural integrity of masonry buildings. *International Journal of Architectural Heritage*. 2012, 6(1), 85-104.
25. Hassan, M. A.; A.A. Ali. Structural integrity of concrete structures. *Journal of Materials and Structures*. 2015, 48(5), 1255-1267.
26. Reed, B.C. The History and Science of the Manhattan Project. Springer Berlin, Heidelberg. 2019. DOI: https://doi.org/10.1007/978-3-662-58175-9
27. Feifer, G. The Battle of Okinawa: The Blood and the Bomb. United States: Lyons Press. 2001.
28. Stimson, H.L.; H.S. Truman. The Decision to Use the Atomic Bomb. *Bulletin of the Atomic Scientists*. 1947, 3:2, 37-67, DOI: 10.1080/00963402.1947.11455840
29. Selden, M. A Forgotten Holocaust: US Bombing Strategy, the Destruction of Japanese Cities and the American Way of War from World War II to Iraq. *The Asia-Pacific Journal*. 2007, 5(5)
30. Obataya, E.; P. Kitin; H. Yamauchi. Bending characteristics of bamboo (Phyllostachys pubescens) with respect to its fiber–foam composite structure. *Wood Sci Technol*. 2007, 41, 385–400. DOI:https://doi.org/10.1007/s00226-007-0127-8
31. Lessard, G.; A. Chouinard. *Bamboo research in Asia*: Proceedings of a workshop held in Singapore, 28-30 May 1980. Ottawa, Ont., IDRC, 1980, p.228.
32. Elert, G. Elasticity Summary. The Physics Hypertextbook. 2021. Obtained from https://physics.info/elasticity/summary.shtml.
33. Huang, Z. Resource-Driven Sustainable Bamboo Construction in Asia-Pacific Bamboo Areas. Germany: Springer International Publishing, 2021.
34. Tewari, D. N. Bamboo in building and construction in Southeast Asia. *Construction and Building Materials*. 2004, 18(6), 447-452.
35. Krawczak, P. Diaphragms in tubes as a measure increasing the energy absorption capacity of structures. *Journal of Theoretical and Applied Mechanics*. 2017, 55(3), 813-823.
36. Marques, R. A.; A.P. Silva. Effect of diaphragms on the strength of steel pipes under axial compression. *Journal of Constructional Steel Research*. 2018, 141, 67-76.
37. Lin, Z.; J. Han; X. Yu; Y. Wang. Effects of diaphragm parameters on ultimate strength of thin-walled tubes. *Thin-Walled Structures.* 2017, 111, 45-54. DOI: https://doi.org/10.1016/j.tws.2016.10.10.003
38. Davidson, J.R. Reliability and structural integrity. NASA *Technical Memorandum*, 1974. 14 p
39. Ciriacy-Wantrup, S.V. Resource Conservation: Economics and Policies. United States: University of California, Division of Agricultural Sciences, Agricultural Experiment Station, 1968.
40. Hu, J.; L. Ma; Z. Li. Numerical study on the effect of diaphragm position on the mechanical behavior of thin-walled tubes. *Thin-Walled Structures*, 2021, 160. DOI: https://doi.org/10.1016/j. tws.2020.107757
41. Xu, S.; J. Deng. Experimental and numerical investigation of thin-walled steel tubes with corrugated diaphragms under axial compression. J*ournal of Constructional Steel Research.* 2016, 120, 162-175. DOI: https://doi.org/10.1016/j.jcsr.2016.01.024
42. Cordero, R.M.; J.C. Polanco; J.A. Montalvo. Structural behavior of cold-formed steel members with circular holes subjected to bending. *Journal of Constructional Steel Research*, 2017,137, 100-110.
43. D. M. Souza; L.M. Correia; E.R.M. Filho. Experimental analysis of composite columns with steel and concrete using full-scale specimens. *Engineering Structures.* 2016, 119, 438-449.
44. ASTM International, Designation D 790-03: Standard test methods for flexural properties of unreinforced and reinforced plastics and electrical insulating materials.
45. Gere, J.M.; B.J. Goodno. Mechanics of Materials. Brief Edition. CENGAGE Learning. 2011.

Author

Sean Jung is a senior at Punahou School. A pursuit in biomedical engineering interests me the greatest. I want to focus on biology and how it could be synthesized to improve the world. I wish to be a part of that conversation.

DOI: 10.36838/v5i6.20